A99-27913 AIAA-99-1979

Subgrid Scale Contribution to Noise Production in Decaying Isotropic Turbulence

Christelle Seror *, Pierre Sagaut †
ONERA, 29 av. de la Division Leclerc, 92322 CHÂTILLON Cedex, FRANCE
Christophe Bailly ‡, Daniel Juvé §
LMFA, ECL, 36 av. Guy de Collongue, BP 163, 69131 ECULLY Cedex, FRANCE

An estimation of the noise generated by subgrid scales provided by LES calculation is performed. The derivation of Navier-Stokes equation to obtain Lighthill's equation is presented for both DNS and LES Navier-Stokes equation. The Lighthill tensor is split into several parts : a high frequency part that is not resolved by LES calculation, the filtered Lighthill tensor computed from basic filtered variables and a subgrid-scale tensor. A DNS of decaying isotropic turbulence is carried out to evaluate the contribution of each term to the noise production. It is confirmed that the high frequency part of the Lighthill's tensor does not contribute significantly to noise production for usual cut-off wavenumber value of LES. The subgrid-scale contribution can not be neglected and requires the use of a subgrid-scale model in order to recover reliable results dealing with the acoustic field. The acoustic contributions computed using a subgrid-scale model of eddy-viscosity type and a subgrid-scale model of scale similarity type is compared to the acoustic contribution of the exact subgrid-scale tensor.

Nomenclature

c_0	= speed of sound
D	= computational length
G	= filter function
k_c	= normalized cut-off wave number
L	= initial integral length scale
M	= Mach number
M_t	= turbulent Mach number
Pr	= Prandtl number
Re	= Reynolds number
Re_λ	= Taylor micro-scale Reynolds number
u^{rms}	= rms velocity
V	= computational domain
$\mathbf{x}$	= observer position
$\mathbf{y}$	= local source position
δ_{ij}	= Kronecker tensor
ϵ	= turbulent dissipation rate
γ	= specific heat ratio
λ	= Taylor micro-scale
μ	= dynamic viscosity
ν	= molecular kinetic viscosity
τ	= initial eddy turn over time

Subscripts

0	= computed a time $t = 0$.

Superscripts

$''$	= high frequency quantity
SGS	= Subgrid Scale quantity

*PhD student
†Scientist Engineer
‡Assistant Professor, Member AIAA
§Professor, Member AIAA

Introduction

Sound generated by turbulence raises many questions of fundamental and engineering interest. Initial work was especially based on analytical and experimental results, but recent progress in Computational Fluid Dynamic (CFD) offer many tools to develop new techniques in Computational Aero-Acoustics (CAA). Since the acoustic source originates in turbulent fluctuations, the resolution of the acoustic field is indeed difficult because of the wide range of spatial and temporal frequencies.[1] A complete knowledge of the unsteady aerodynamic field can not then be reached in practical configurations of interest. A steady statistical description of the turbulent flow has long been used[2,3] before numerical simulations were carried out to compute the aerodynamic field.[4]
Direct Numerical Simulation (DNS),[5] unsteady Reynolds Averaged Navier-Stokes simulations (RANS),[6] semi-deterministic modelling (SDM)[7,8] or, as detailed in this paper, Large Eddy Simulation (LES),[9,10] are actually used to compute the acoustic source (i.e. the unsteady flow field). DNS approach does not allow to compute high Reynolds number turbulent flows that have to be dealt with in practice. As noise radiated from turbulent flow generates especially from large scale motion[9] LES which is based on the resolution of low wavenumber components (referred to as $\bar{u}$) and on the parametrization of high wavenumber components (referred to as u'') of turbulent quantities offers a very attractive issue to resolve such problems. CAA offers then many possibilities to calculate the sound field radiated by turbulent fluctuations : Lighthill's analogy[11,12] retained for the present work, a third-order wave equation namely

Lilley's equation[13] or the linearized Euler's equations. Each of these descriptions requires the knowledge of the aerodynamic field. Lighthill's analogy, which is based on the resolution of Lighthill's equation derived from the compressible Navier-Stokes equations, was the first attempt to estimate the sound radiated from a finite region of turbulent flow. This method is a very powerful and general approach to compute the acoustic radiated field although it has the limitation of assuming that refraction effect cannot be taken into account. Using this analogy, the pressure generated by a turbulent flow is expressed as a function of the Lighthill's tensor $T_{ij} \approx \rho u_i u_j$. In LES calculations only the filtered variables $\widetilde{u}_i$ are available and so, Lighthill's tensor can not be computed in its complete form. A Lighthill's tensor $T_{ij}^{LES} = \overline{\rho}\ \widetilde{u}_i \widetilde{u}_j$ calculated with the basic filtered variables is often used.[9,10] The aerodynamic field does not contain all frequencies available but only the low frequency part of the field. The importance of this last one may be revelant for aeroacoustic computations and must be estimated .

This paper addresses the new problem of the evaluation and modelling of the contribution of the unresolved scales to the radiated noise production, when Lighthill's analogy is employed together with LES, namely a Hybrid LES method. The governing equations for DNS and Lighthill's analogy (i.e Hybrid DNS) are first presented and exented to the case of Hybrid LES approach. The second section is devoted to the evaluation of the subgrid and high frequency contributions to the complete Lighthill tensor, on the ground of *a priori* tests performed in the decaying isotropic turbulence case. The third section deals with the parametrization of the subgrid scale noise production, and results of *a priori* tests are discussed. Conclusions are presented in the last section .

Mathematical formulation

Governing equations for hybrid DNS

For an ideal gas, equations of motion : continuity ,momentum and energy conservation equations can be recasted in the following form :

$$\frac{\partial}{\partial t}\rho + \frac{\partial}{\partial y_i}\rho u_i = 0 \qquad (1)$$

$$\frac{\partial}{\partial t}\rho u_i + \frac{\partial}{\partial y_j}\rho u_i u_j = \frac{\partial}{\partial y_i}(-p\delta_{ij} + \sigma_{ij}) \qquad (2)$$

$$\frac{\partial}{\partial t}E + \frac{\partial}{\partial y_i}((E+p)u_i) = \frac{\partial}{\partial y_i}(\sigma_{ij}u_j) - \frac{\partial}{\partial y_i}Q_i \qquad (3)$$

where ρ, u_i, p, E are respectively the density, the velocity components, the thermodynamic pressure and the total energy.
The viscous stress tensor σ_{ij} is defined as,

$$\sigma_{ij} = -\frac{2}{3}\frac{\mu}{Re}\frac{\partial}{\partial y_k}u_k\ \delta_{ij} + \frac{\mu}{Re}(\frac{\partial}{\partial y_i}u_j + \frac{\partial}{\partial y_j}u_i) \qquad (4)$$

The heat flux vector Q_i is written as follows :

$$Q_i = -\frac{\mu}{(\gamma-1)RePrM^2}\frac{\partial}{\partial y_i}\Theta \qquad (5)$$

where Θ denotes the temperature. For an air flow, the specific heat ratio is $\gamma = 1.4$ and the Prandtl number Pr is equal to 0.7
These equations must be supplemented with the equation of state :

$$p = \frac{1}{\gamma M^2}\rho\Theta \qquad (6)$$

One of the first attempts to estimate the sound radiated from a finite region of turbulent flow was proposed by Lighthill.[11,12] The combination $\frac{\partial}{\partial t}(1) - \frac{\partial}{\partial y_i}(2)$ of these equations leads to Lighthill's wave equation for the density :

$$\frac{\partial^2}{\partial t^2}\rho - c_o^2\frac{\partial^2}{\partial y_i y_i}\rho = \frac{\partial^2}{\partial y_i \partial y_j}T_{ij} \qquad (7)$$

where c_0 is the constant speed of sound in the ambient medium and the Lighthill's tensor T_{ij} is defined as follows :

$$T_{ij} = \rho u_i u_j + (p - c_0^2\rho)\delta_{ij} - \sigma_{ij} \qquad (8)$$

For high Reynolds number the viscous stress tensor σ_{ij} in Lighthill's tensor expression can be neglected. For low turbulent Mach number the pressure perturbations are assumed to be nearly isentropic and the acoustic pressure can then be written as : $p = c_0^2\ \rho$. Under these assumptions the Lighthill's tensor simplifies to :

$$T_{ij} = \rho u_i u_j \qquad (9)$$

The solution of equation (7) is exact only for an homogeneous medium at rest and refraction effects are not taken into account.[1] In order to obtain an integral formulation, the Green function is required.

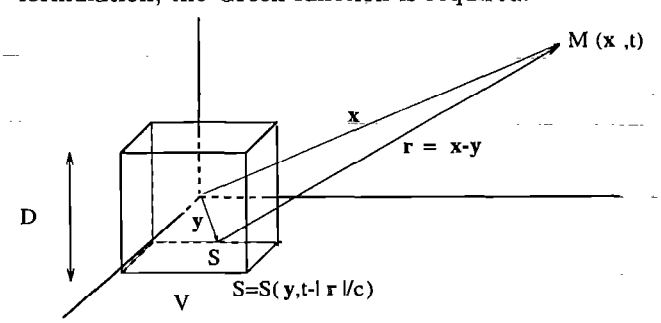

Fig. 1 Geometry of sound source radiation. V = Volume of turbulent fluid, M = observer position, $D = 2\pi$

Thus the fluctuating density[9,19] can be expressed as a function of Lighthill's tensor :

$$\rho'(x,t) = \frac{1}{4\pi c_0^4}\frac{x_i\ x_j}{x^3}\int_V [\frac{\partial^2}{\partial t^2}T_{ij}] - < [\frac{\partial^2}{\partial t^2}T_{ij}] > d^3y \qquad (10)$$

where the symbol [.] denotes the evaluation at the retarded time $t - \frac{r}{c_0}$ where $\mathbf{r} = \mathbf{x} - \mathbf{y}$ is the vector joining the source point $\mathbf{y}$ to the observation point $\mathbf{x}$, as shown in Fig. 1 and $< . >$ denotes statistical average.
As soon as the aerodynamic field is known, the fluctuating acoustic density can be computed. For high Reynolds numbers, a direct numerical simulation can not be carried out because of the very high computational cost, and then, statistical models are used to account for a part of the turbulent fluctuations. The LES offers the possibility to compute high Reynolds number turbulent flows by resolving large eddies and parametrizing small eddies. The description of the governing equation when LES and Lighthill's analogy are used together is presented in the following section.

Extension to LES

In Large-Eddy Simulation of compressible turbulent flows, any quantity F in the flow domain V can be decomposed into a resolved or filtered part $\overline{F}$ and an unresolved or subgrid part f through the application of a low-pass convolution filter :

$$F = \overline{F} + f \tag{11}$$

with

$$\overline{F}(\mathbf{y}) = \int_V G_\Delta(\mathbf{y} - \xi) F(\xi) d\xi \tag{12}$$

where G_Δ is the filter kernel, and $\Delta = \pi/k_c$ the characteristic cut-off length scale. The filter kernel G_Δ is a spatial filter (usually a sharp cut-off filter in Fourier space or a Gaussian filter) of width equal to the grid spacing. When dealing with variable density flows, the mass-weigthed variables $\widetilde{F}$ are used following Favre,[14] with:

$$\widetilde{F} = \frac{\overline{\rho F}}{\overline{\rho}} \tag{13}$$

Thus, the quantity F is now decomposed as :

$$F = \widetilde{F} + F'' \tag{14}$$

Using this definition the Favre filtered continuity and momentum equations are :

$$\frac{\partial}{\partial t}\overline{\rho} + \frac{\partial}{\partial x_j}\overline{\rho}\,\widetilde{u}_j = 0 \tag{15}$$

$$\frac{\partial}{\partial t}\overline{\rho}\,\widetilde{u}_i + \frac{\partial}{\partial y_j}\overline{\rho}\,\widetilde{u}_i\,\widetilde{u}_j + \frac{\partial}{\partial y_i}\overline{p} = \frac{\partial}{\partial y_j}\widetilde{\sigma_{ij}} - \frac{\partial}{\partial y_j}\tau_{ij} \tag{16}$$

The term τ_{ij} is a subgrid quantity resulting from the non-linearity of the convective terms and is defined as :

$$\tau_{ij} = \overline{\rho}(\widetilde{u_i u_j} - \widetilde{u}_i\,\widetilde{u}_j) \tag{17}$$

Following Vreman approach[15] and according to Brandsma assumptions,[16] the Favre filtered energy equation is straightforward.

The filtered Lighthill's equation can be obtained in two ways: by operating the combination of the filtered continuity equation and filtered momentum equation, i.e. $\frac{\partial}{\partial t}(15) - \frac{\partial}{\partial y_i}(16)$, or by filtering the Lighthill's equation (7). In both cases, the resulting equation for resolved (or filtered) density is:

$$\frac{\partial^2}{\partial t^2}\overline{\rho} - c_o^2\frac{\partial^2}{\partial y_i y_i}\overline{\rho} = \frac{\partial^2}{\partial y_i \partial y_j}\widetilde{T_{ij}} \tag{18}$$

where the filtered Lighthill tensor $\widetilde{T_{ij}}$ which represents the production of resolved acoustic fluctuations is then given by :

$$\widetilde{T_{ij}} = \overline{\rho}\,\widetilde{u_i u_j} \tag{19}$$

The filtered Lighthill's tensor differs from T_{ij} by T''_{ij}, the high frequency part of the complete Lighthill's tensor which is not resolved in LES calculations. The resulting decomposition of T_{ij} is given by :

$$T_{ij} = \widetilde{T_{ij}} + T''_{ij} \tag{20}$$

Since the basic variables of LES calculations are $\overline{\rho}$ and $\widetilde{u}_i$, the source term $\widetilde{T}_{ij}$ can not be directly computed and must be approximated by $T_{ij}^{LES} = \overline{\rho}\,\widetilde{u}_i\widetilde{u}_j$ with an inherent error $T_{ij}^{S.G.S}$ which is actually the subgrid scale tensor τ_{ij} defined in equation (17) :

$$\widetilde{T_{ij}} = T_{ij}^{LES} + T_{ij}^{S.G.S} = \overline{\rho}\,\widetilde{u}_i\widetilde{u}_j + \tau_{ij} \tag{21}$$

The final decomposition for the full Lighthill's tensor is then written as :

$$T_{ij} = T_{ij}^{LES} + T_{ij}^{SGS} + T''_{ij} \tag{22}$$

In order to get reliable far-field noise prediction using LES calculations, the subgrid scale tensor appears naturally as a source term in the expression of the acoustic fluctuating pressure, and must be evaluated to assess the accuracy of a prediction of the far-field noise from LES simulations.

A priori evaluation of the subgrid acoustic source

Numerical simulation description and validation

A priori tests were carried out to estimate the subgrid contributions to radiated noise considering freely decaying isotropic turbulence. This case corresponds to a self-similar statistically non-stationary solution, but does not require the use of a random forcing term whose acoustic properties are unknown, as the forced isotropic turbulence case does.

Direct Numerical Simulations were performed on a $N^3 = 72^3$ uniform spatial grid using a fourth-order centered scheme for the convective terms, a second-order centered scheme for the viscous terms and a third-order Runge-Kutta scheme for the integration in time. The initial parameters of the simulation are reported in Table 1.

N	Re_λ	M_t	L_0	λ_0	η_0
72	19	0.3	0.64	0.5	0.03

Table 1 Numerical and flow parameters for DNS calculations

In the simulation the Taylor microscale Reynolds number $Re_\lambda = \lambda_0 K_0/\nu$ is equal to 19. and the turbulent Mach number $M_t = u_0^{rms}/c_0$ is equal to 0.3. The initial velocity field is chosen to be solenoidal. This initial condition and the low value of the Mach number value ensure that the flow will follow a quasi-incompressible behavior,[17] allowing the use of the reduced form of the Lighthill tensor given by equation (9).

The initial energy spectrum is given by :

$$E(k) = k^4 \exp\left(-2k^2/k_0^2\right) \quad \text{with} \quad k_0 = 4 \qquad (23)$$

At the beginning of the simulation, the mesh size Δy is such that $\Delta y/\eta_0 = 2.95$ where $\eta_0 = \left(\nu^3/\epsilon_0\right)^{1/4}$ is the Kolmogorov length scale at the initial time and is in good agreement with DNS resolution requirements. Since we are dealing with freely decaying turbulence, the ratio $\Delta y/\eta$ will decrease as the Kolmogorov scale increases, ensuring that the resolution is accurate enough to capture all the relevant turbulent fluctuations during the whole simulation. Turbulence statistics presented hereafter are obtained by performing a statistical average over the computational domain and are presented as a function of the dimensionless time $t^* = \frac{t}{\tau_0}$, where $\tau_0 = L_0/u_0^{rms}$ is the initial large eddy turnover time. The normalized turbulent dissipation rate $\epsilon(t^*)/\epsilon_0$ plotted in Fig. 2 increases during the initial transient due to the generation of small-scale fluctuations through the non-linear kinetic energy cascade process, and finally decays in the absence of external forcing once the spectrum is fullfilled. The time evolution of the Taylor microscale Reynolds number Re_λ is represented in Fig. 3. The end of the acoustic calculations is chosen such as the Taylor microscale number has decreased by a factor of 3 from its initial value, Re_λ being too small at latter time to ensure a realistic representation of turbulence dynamics. The skewness factor of the velocity derivative $S_k = < (\partial u/\partial x)^3 > / < (\partial u/\partial x)^2 >^{3/2}$ supplies a measure of the non-linear vortex stretching. The experimental value for isotropic turbulence of S_k is given to be -0.4, while simulations give $S_k \approx -0.5$.[18] Results presented on Fig. 4 shows that for present calculations the skewness asymptotes to the value $S_k \approx -0.48$, leading to a satisfactory agreement.

As acoustic results are revelant when the decay of turbulence is autosimilar,[19] the acoustic calculation is initialized at this time in order to avoid spurious non-equilibrium effects in the calculation of acoustic source terms. The kinetic energy spectrum computed at time

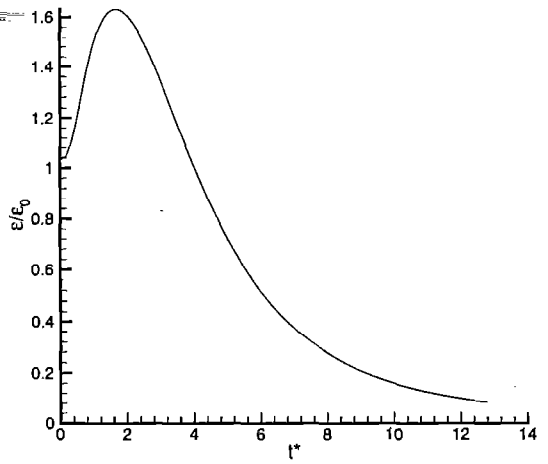

Fig. 2 Normalized dissipation ϵ/ϵ_0 time history

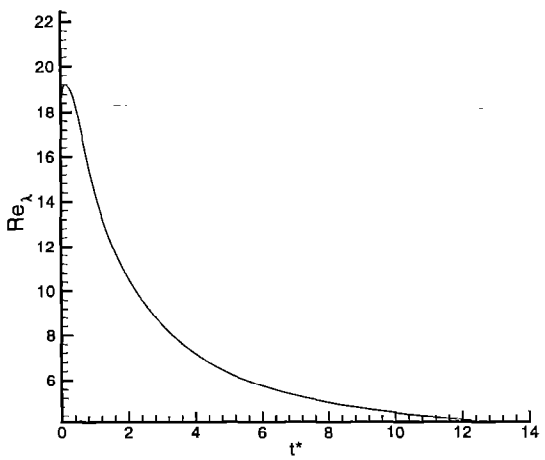

Fig. 3 Taylor microscale Reynolds number Re_λ time history

$t^* = 3.55$ is plotted in Fig. 5. A $k^{-5/3}$ slope is recovered on the interval $5 \leq k \leq 10$, in agreement with Moin and Mahesh statement[20] that a decade-wide inertial range is found only for $Re_\lambda \geq 100$. These results demonstrate the good quality of the simulation, which is suitable for *a priori* testing.

Acoustic quantities computation

The fluctuating pressure is computed[9,19] using equation (10)

$$p'(x,t) = \frac{1}{4\pi c_0^2} \frac{x_i\, x_j}{x^3} \int_V [\frac{\partial^2}{\partial t^2} T_{ij}] - < [\frac{\partial^2}{\partial t^2} T_{ij}] > d^3y \qquad (24)$$

and the acoustic intensity is computed[9] as follows :

$$I = \frac{< (p'(x,t))^2 >}{\rho_0 c_0} \qquad (25)$$

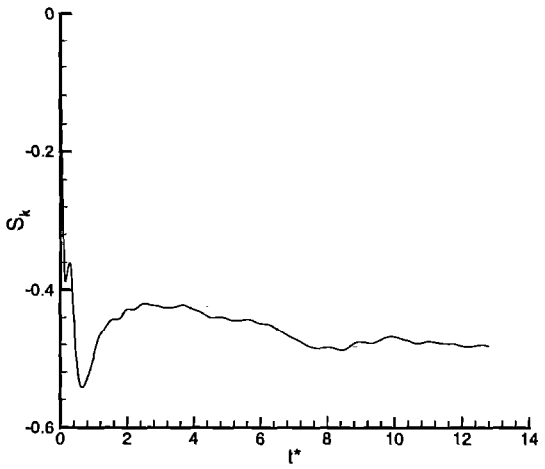

Fig. 4 Skewness S_k time history

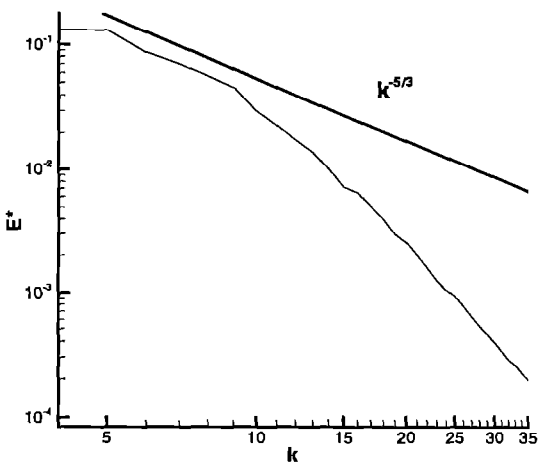

Fig. 5 Normalized energy spectrum defined as : $E^* = \frac{E(k)}{\int_0^\infty E(k)\,dk}$ at time $t^* = 3.55$

The ensemble average <> is computed over 6 different, but statistically equivalent, simulations and for each simulation with 24 different observer points located at the same distance from the center of the computational domain V, yielding 144 samples. It was checked that this process ensures the convergence of statistical moments. The radiated acoustic pressure is computed at observer points distributed on 6 planes P_i, $i = 1, 6$ parallel to the faces of the volume of turbulent fluid. Each plane P_i is located at the same distance, $x = 10D$ from the center of the computational domain, where D is defined in Fig. 1, and each plane contains 4 observer points . Since the considered computational time step is $\Delta t = 0.01\ D/c_0$, only the time delay between planes perpendicular to the direction of $\mathbf{x}$ is taken into account to compute the retarded time in expression (10). The 4 observer points on each plane P_i are distributed such as the time delay difference between these observer points is less than the time step and is neglected.

Acoustical results

The acoustic fluctuating pressure computed from DNS data using equation (24) is displayed in Fig. 6 as a function of time at an observer position. The pressure signal observes a general decay process induced by the decrease of the acoustic source term $\frac{\partial^2}{\partial t^2} T_{ij}$ associated to the kinetic energy decay.

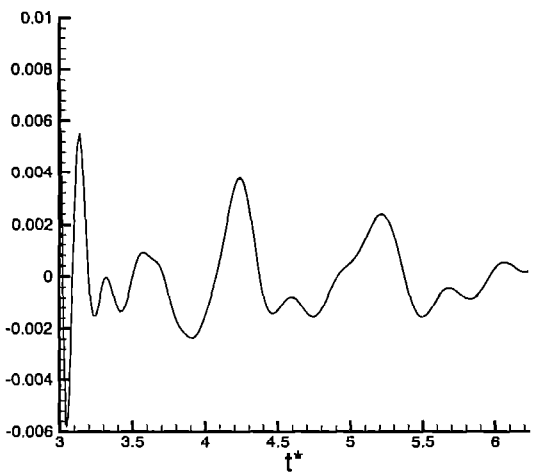

Fig. 6 Fluctuating acoustic pressure calculated from DNS data

In order to access the exact acoustic pressure respectively resulting from the subgrid scale and the high frequency part of the source term, Lighthill's tensors $\widetilde{T}_{ij}$ and T_{ij}^{LES} have been computed from DNS data according to equation (12). Two filters have been considered, namely a Gaussian filter and a sharp spectral cut-off filter, whose associated kernel in physical space G_Δ and transfer function $\hat{G}$ are respectively:

$$G_\Delta(\mathbf{y}-\xi) = \left(\frac{6}{\pi\Delta^2}\right)^{\frac{1}{2}} \exp\left(\frac{-6|\mathbf{y}-\xi|}{\Delta^2}\right)^2$$
$$\hat{G}(k) = exp\left(\frac{-\Delta^2 k^2}{24}\right) \qquad (26)$$

$$G_\Delta(\mathbf{y}-\xi) = \frac{sin(k_c(\mathbf{y}-\xi))}{k_c(\mathbf{y}-\xi)}$$
$$\hat{G}(k) = \begin{cases} 1 & \text{if } |k| \le k_c = \pi/\Delta \\ 0 & \text{else} \end{cases} \qquad (27)$$

The Gaussian filter (26) induces a smooth separation between resolved and subgrid quantities, resulting in a non-zero contribution of low frequencies to the latters. On the contrary, the sharp spectral cut-off filter (27) prevents any contribution of low frequencies to SGS terms. The effect of the two filters has been

investigated as a function of the normalized cut-off wavenumber k_c. Results are presented for values of the cut-off wavenumber k_c reported in Table 2. The ratio between the characteristic cut-off length-scale and respectively characteristic flow length scales respectively η_0, λ_0 and L_0 has also been reported in the Table 2 . Δ/η_0 indicates the resolution of the mesh in terms of the Kolmogorov length scale. LES models ensure reliable results for the aerodynamic field when the mesh size used in LES computations is such as $\Delta \approx \lambda$. This condition ensures that the cut-off wave number k_c associated to Δ is contained in the dissipation spectrum. As the integral length scale is the characteristic large scale of the turbulent flow, Δ is required to be less than L_0 to ensure a good resolution of the large eddies. Table 2 indicates that cut-off wave number values $k_c \geq 8$ can then be used to compute the flow field.

k_c	4	6	8	10	12	14	16	18	20	22
Δ/η_0	26.17	17.45	13.10	10.47	8.73	7.48	6.54	5.82	5.24	4.76
Δ/λ_0	1.57	1.05	0.80	0.63	0.52	0.45	0.39	0.35	0.31	0.29
Δ/L_0	1.23	0.89	0.61	0.49	0.41	0.35	0.30	0.27	0.25	0.22

Table 2 Values and characteristic of k_c and Δ

First, the difference between acoustic values computed from DNS data with the exact tensor T_{ij}, and acoustic values obtained from LES data associated to $\widetilde{T_{ij}}$ has been investigated. This preliminary study allows the analysis of the acoustic properties of the high frequency part of the acoustic source T''_{ij}. In order to bring out the importance of the high frequency part of the acoustic source, the intensity ratio $I''/I = (I - \widetilde{I})/I$ is computed as a function of k_c (Fig. 7), where $\widetilde{I}$ and I are the acoustic intensities respectively associated to the filtered source term $\widetilde{T}_{ij}$ and the full Lighthill tensor T_{ij}.

Two different times are considered: the first one $t^* = 4.74$ corresponds to a maximal contribution of the subgrid scales and the second one, $t^* = 5.33$, to a small contribution of these modes. For both times, the intensity ratio tends rapidly to zero and the intensity of the unresolved noise is less than 10% of the total intensity for $k_c \geq 8$. Since the unresolved noise is found to be small for both filters with cut-off wavenumber $k_c > 8$, it is deduced that exact LES calculations using $\widetilde{T_{ij}}$ can be suitable to compute the acoustic source and that the acoustic features of the considered turbulent flow are connected to the low frequency part of the source. These results are in agreement with those obtained by Witkowska *et al.*[9] concerning noise generation process in isotropic turbulence.

Additional *a priori* tests were carried out to estimate the low-frequency noise generated by the SGS stress tensor T_{ij}^{SGS}. To compare fluctuating acoustic

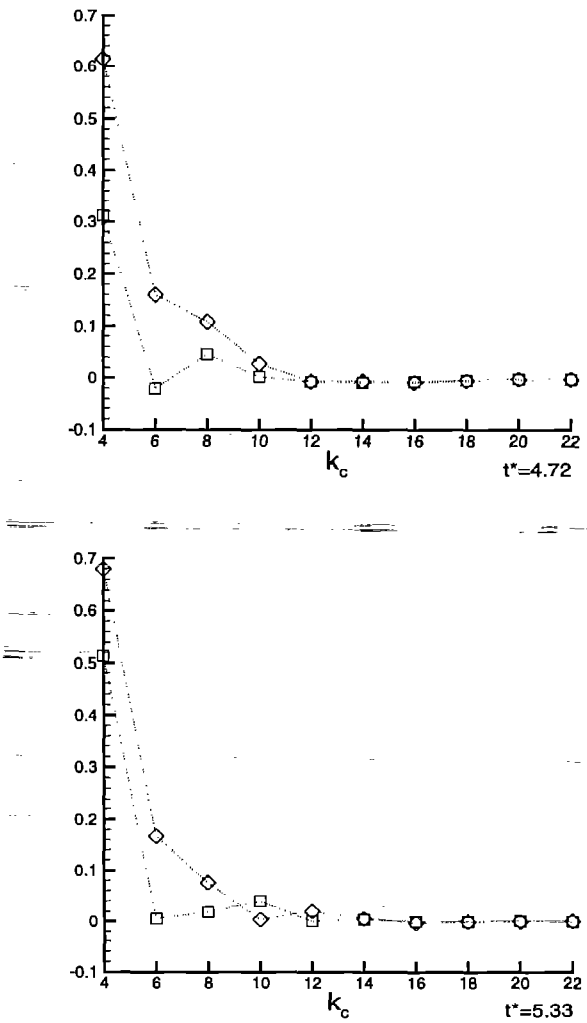

Fig. 7 Evolution of the intensity of the unresolved noise by LES calculation I''/I as a function of the cut-off wavenumber k_c for two different times. □, Sharp cut-off filter and ◇, Gaussian filter

pressures p', $\widetilde{p'}$, p'^{LES} associated respectively to source terms T_{ij}, $\widetilde{T_{ij}}$ and T_{ij}^{LES}, the spectral cut-off filter and the Gaussian filter were used to filter the DNS flow field. For the lowest usual value of k_c in LES ($k_c = 8$) (Fig. 8.a, Fig. 8.b) discrepancies between the fluctuating acoustic pressure p', $\widetilde{p'}$, p'^{LES} are observed, considering both the amplitude and the phase of the signal. This result indicates that the use of LES calculations to compute the acoustic source term cannot be used for $k_c \leq 8$ because the unresolved acoustic source term remains significant.

This unresolved noise contribution is reduced when larger values of k_c are considered (see Fig. 9.a and Fig. 9.b). Nevertheless, the discrepancies between $\widetilde{p'}$ and p'^{LES} is still large, indicating that the effect of the subgrid scale must be taken into account.
In all cases the discrepancies between the fluctuating acoustic pressures p', $\widetilde{p'}$, p'^{LES} are more significant us-

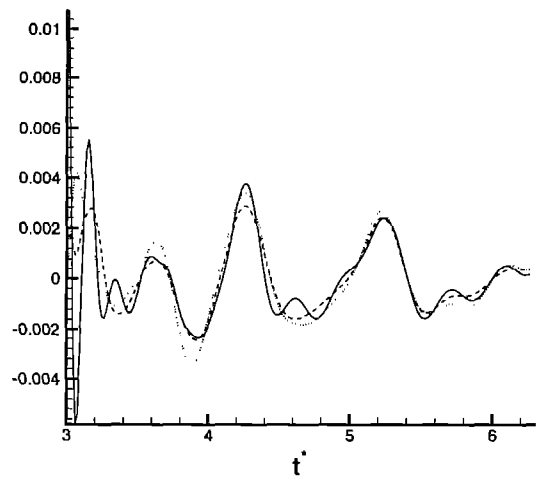

(a)

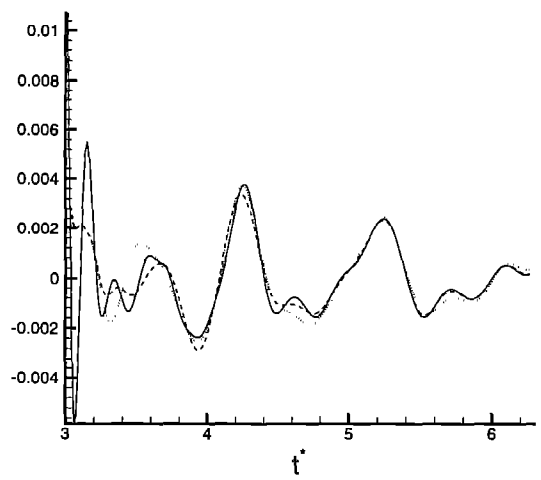

(b)

Fig. 8 Comparison between the fluctuating acoustic pressures — p', - - $\widetilde{p'}$, $\cdots$ p'^{LES} respectively computed from the exact Lighthill's tensor T_{ij} and from filtered Lighthill's tensors $\widetilde{T}_{ij}$ and T_{ij}^{LES}. (a) - $k_c = 8$ - Gaussian filter (b) - $k_c = 8$ - Spectral cut-off filter

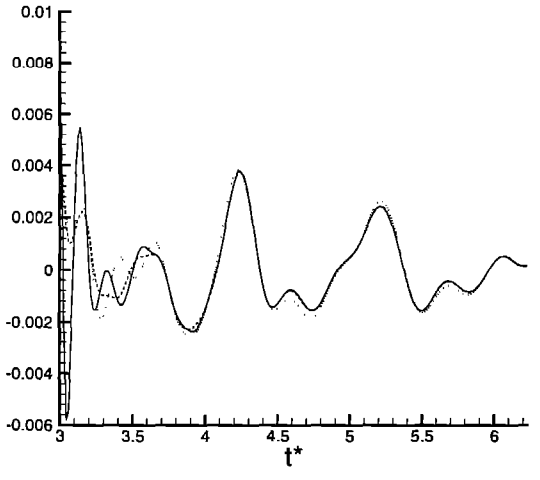

(a)

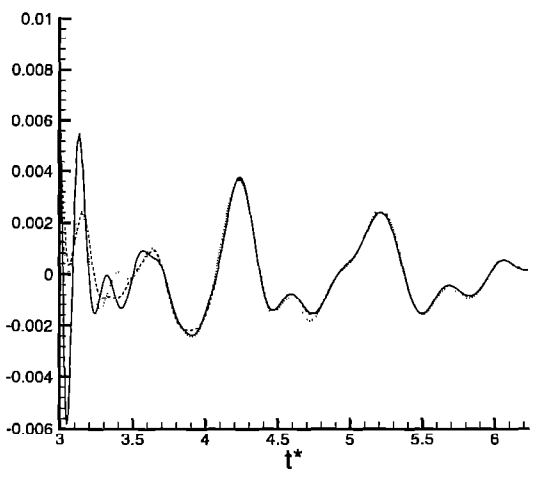

(b)

Fig. 9 Comparison between the fluctuating acoustic pressures — p', - - $\widetilde{p'}$, $\cdots$ p'^{LES} respectively computed from the exact Lighthill's tensor T_{ij} and from filtered Lighthill's tensors $\widetilde{T}_{ij}$ and T_{ij}^{LES}. (a) - $k_c = 12$ - Gaussian filter (b) - $k_c = 12$ - Spectral cut-off filter

ing the Gaussian filter than the spectral cut-off filter. This can be explained by the non-local character of the Gaussian filter in the Fourier space, which allows large eddies to contribute to the subgrid scales, resulting in an increase of the contribution of the subgrid scale to the noise generation process.

The intensity ratio $I_{SGS}/\widetilde{I} = (\widetilde{I} - I_{LES})/\widetilde{I}$ (where I_{SGS} and I_{LES} are respectively deduced from T_{ij}^{SGS} and T_{ij}^{LES}) is reported as a function of k_c for the two selected filters on Fig. 10 at the two different times considered previously. The subgrid scale contribution to the resolved acoustic intensity is seen to be important (i.e. at least 10 % of the total) for cut-off wavenumbers $k_c \leq 12$ at time $t^* = 4.74$. As expected, that contribution is much less significant at $t^* = 5.33$, but the error is still concentrated on modes $k \leq 12$. As already noticed on the fluctuating acoustic pressure, the Gaussian filter induces a larger contribution of the subgrid modes, due to its non-local character. These results indicate in the present computation that the use of LES calculations to compute the acoustic radiation will lead to an unreliable prediction if the spectral cut-off wave number is such as $k_c \leq 8$ which corresponds to a ratio $\Delta/L_0 > 0.6$. For $8 < k_c \leq 12$ the source term $T_{ij}^{S.G.S.}$ must be taken into account in order to recover subgrid-scale effects. Finally for value of k_c greater than 12, i.e $\Delta/L_0 < 0.4$, the subgrid-scale effect are not important and the computation of the

acoustic source term can be carried out without taking into account other effects.

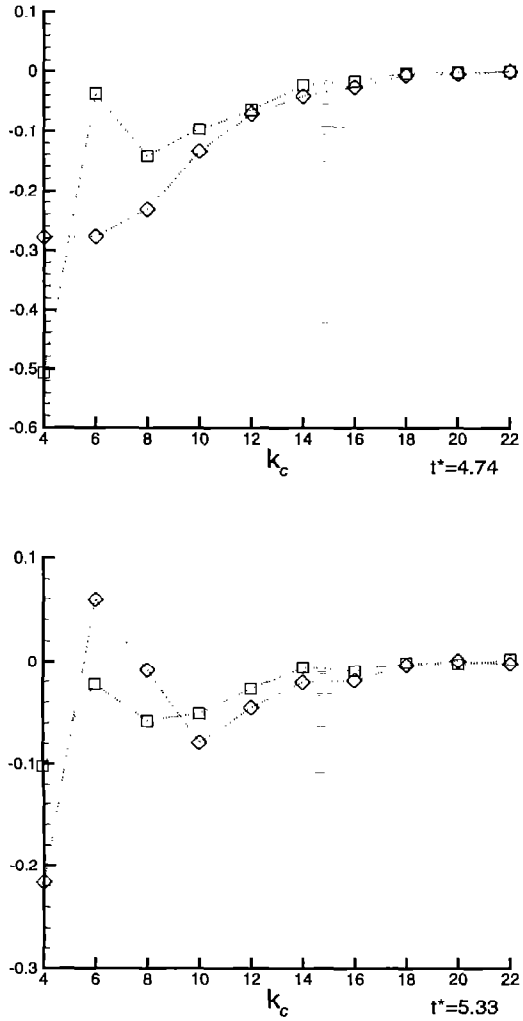

Fig. 10 Evolution of the subgrid scale intensity $I^{SGS}/\widetilde{I}$ as a function of the cut-off wavenumber k_c for two different times. □, Sharp cut-off filter and ◇, Gaussian filter

Parametrization of Lighthill's subgrid scale tensor

In previous section it has been demonstrated that the subgrid scale tensor in Lighthill's equation must be taken into account in order to recover reliable results. Many ways of modelling the subgrid scale tensor τ_{ij} have already been developped.[21,22] As the Lighthill's subgrid scale tensor T_{ij}^{SGS} has the same expression, the usefulness of these SGS models to correct acoustic variables calculated from T_{ij}^{LES} is now investigated. If SGS models were perfect, the acoustic field associated to $\widetilde{T}_{ij}$ could be recovered from the LES computation. The exact and approximate subgrid scale fluctuating acoustic pressure (p'^{SGS} and $\mathcal{P}'^{SGS}$) respectively computed as a function of T_{ij}^{SGS} and m_{ij} (where m_{ij} is the SGS model for T_{ij}^{SGS}) are written as follows:

$$p'^{SGS}(x,t) = \frac{1}{4\pi c_0^2}\frac{x_i\,x_j}{x^3}\int_V [\frac{\partial^2}{\partial t^2}T_{ij}^{SGS}] - < [\frac{\partial^2}{\partial t^2}T_{ij}^{SGS}] > d^3y \tag{28}$$

$$\mathcal{P}'^{SGS}(x,t) = \frac{1}{4\pi c_0^2}\frac{x_i\,x_j}{x^3}\int_V [\frac{\partial^2}{\partial t^2}m_{ij}] - < [\frac{\partial^2}{\partial t^2}m_{ij}] > d^3y \tag{29}$$

The corrected fluctuating acoustic pressure is then given by : $\mathcal{P}'(x,t) = p'^{LES}(x,t) + \mathcal{P}'^{SGS}(x,t)$ and must be compared to $\widetilde{p'}(x,t)$. The resulting acoustic intensity is evaluated as $I_{LES} + \mathcal{I}_{SGS} = < \mathcal{P}'^2(x,t) > /(\rho_0 c_0)$, where $\mathcal{I}_{SGS}$ is related to the *parametrized* SGS tensor (while I^{SGS} is computed using the *exact* SGS tensor). In order to estimate the intensity correction given by the SGS model, the ratio $(\widetilde{I} - (I_{LES} + \mathcal{I}_{SGS}))/\widetilde{I}$ will be compared to $I_{SGS}/\widetilde{I}$. The ratio can also be written as $(I_{SGS} - \mathcal{I}_{SGS})/\widetilde{I}$ and is identically zero when the exact subgrid-scale intensity is recovered. *A priori* tests based on the Gaussian filter for two selected SGS models are now discussed.

Subgrid scale models of eddy-viscosity type

Subgrid scale models using an eddy-viscosity are based on the hypothesis that the deviatoric part of the τ_{ij} is locally aligned with the filtered deviatoric part of the strain tensor, while the normal stresses are assumed to be isotropic and are thus represented through a subgrid scale kinetic energy. A compressible Smagorinsky's model[23] has been used to compute the Lighthill's subgrid-scale tensor is written as follows :

$$m_{ij} - \frac{1}{3}m_{kk}\,\delta_{ij} = -\nu^{SGS}\left(\widetilde{S}_{ij} - \frac{1}{3}\widetilde{S}_{kk}\delta_{ij}\right) \qquad \nu^{SGS} = \overline{\rho}(C_S\Delta)^2\,|\widetilde{S}| \tag{30}$$

$$m_{kk} = 2C_I\overline{\rho}\Delta^2\,|\widetilde{S}|^2 \tag{31}$$

where $\widetilde{S}_{ij} = \frac{1}{2}\left(\frac{\partial}{\partial y_j}\widetilde{u}_i + \frac{\partial}{\partial y_i}\widetilde{u}_j\right)$.
The Smagorinsky constant C_S is taken equal to $C_S = 0.18$, which is the classically admitted value for isotropic turbulence. As the trace of tensor m_{ij} is negligeable in the present case because of the quasi-incompressible behavior of the simulated turbulence,[24,25] it is assumed that $C_I = 0$. The fluctuating acoustic pressure p'_{LES} has been corrected by adding the fluctuating pressure $\mathcal{P}'^{SGS}$ (Fig. 11) computed with the model (30). The comparison between $\widetilde{p'}$ and $p'^{LES} + \mathcal{P}'^{SGS}$ shows that the use of this model leads to very large errors on the predicted acoustic field, on both the phase of the signal and its amplitude. This trend is assessed by looking at the evolution of the intensity ratio $(I_{SGS} - \mathcal{I}_{SGS})/\widetilde{I}$ as a function of k_c (Fig. 12), which is related to the error introduced by the parametrization of the Lighthill's subgrid scale tensor. The Smagorinsky model leads to a very large

overprediction (up to 100 %) of the noise generated by subgrid modes, resulting in worst results than an uncorrected evaluation (i.e. taking $m_{ij} = 0$). In addition, tion of the acoustic source term $\partial^2 T_{ij}^{SGS}/\partial t^2$.

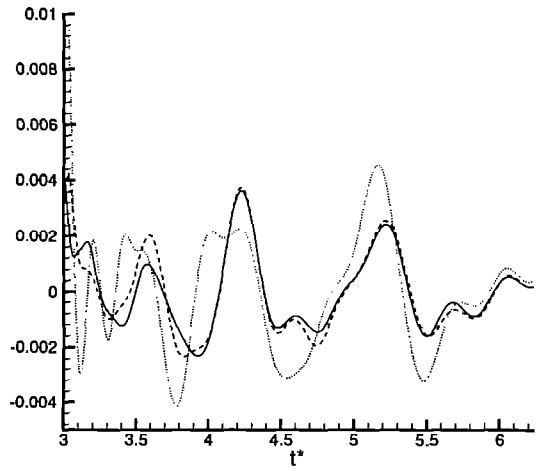

(a)

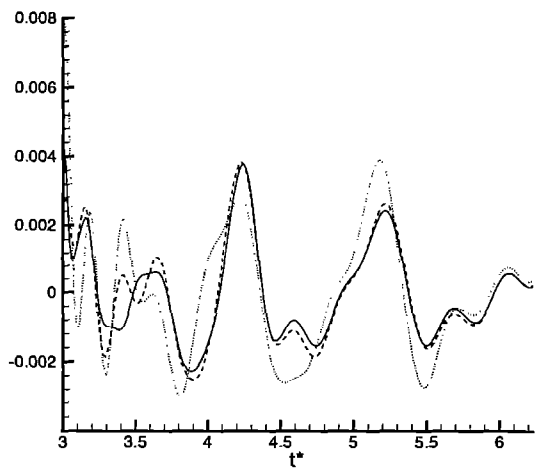

(b)

Fig. 11 Comparison between the fluctuating acoustic pressures — $\widetilde{p'}$, - - p'_{LES} and $\cdots$ $p'_{LES}+\mathcal{P}'_{SGS}$, where p'_{SGS} has been computed from Smagorinsky model for the Gaussian filter. (a) - $k_c = 10$, (b) - $k_c = 12$

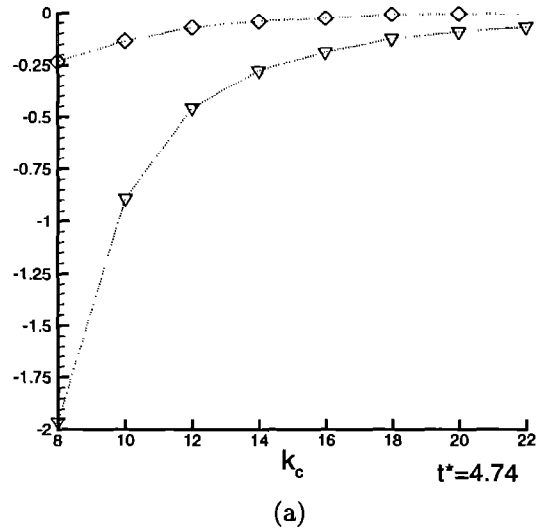

(a)

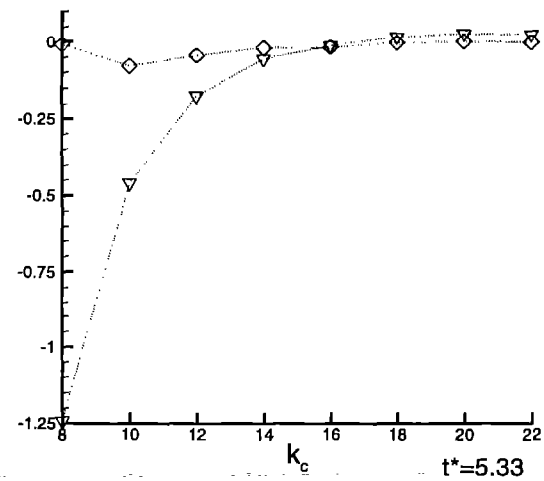

(b)

Fig. 12 Comparison between the subgrid scale intensity $I_{SGS}/\widetilde{I}$, $\diamond$, and the $(I_{SGS} - \mathcal{I}_{SGS})/\widetilde{I}$, $\triangledown$, where $\mathcal{I}_{SGS}$ has been computed from Smagorinsky's model with a Gaussian filter as a function of cut-off wave number k_c .

eddy-viscosity subgrid-scale models are designed to ensure a drain of the resolved kinetic energy but does not restitute the characteristic elements (eigenvalues, eigenvector) of the subgrid-scale tensor. More over the subgrid scale source term is a quadripolar acoustic term in its exact form and eddy-viscosity subgrid-scale models introduce the gradient of the velocity and then makes the parametrization of the subgrid scale source term non quadripolar. Consequently, eddy-viscosity subgrid-scale models fail in the parametrization of subgrid-scale tensor T_{ij}^{SGS} in Lighthill's equation and are not expected to lead to a satisfactory representa-

Subgrid scale models of scale similarity type

Subgrid scale models of scale similarity type are based on the hypothesis that the interactions between grid-scale and the subgrid-scale modes occur especially between the smallest grid-scale modes and the largest subgrid-scale ones, and that SGS stresses can be evaluated through an extrapolation in frequency.

The Bardina's scale similarity model[26,27] has been used to compute the Lighthill's subgrid-scale tensor. It is based on the hypothesis that the interactions between grid-scale and the subgrid-scale modes occur especially between the smallest grid-scale modes and the largest subgrid-scale ones, and that SGS stresses can

be evaluated through an extrapolation in frequency. The corresponding model for the subgrid-scale tensor is written as :

$$m_{ij} = \overline{\rho}(\widetilde{\widetilde{u}_i \widetilde{u}_j} - \widetilde{\widetilde{u}}_i \widetilde{\widetilde{u}}_j) \qquad (32)$$

Results dealing with the fluctuating acoustic pressure (Fig. 13) show that the model does not induce spurious acoustic pressure fluctuations and provides significant improvements when discrepancies between $\widetilde{p'}$ and p'^{LES} are important (e.g. for $t^* \approx 3.55$.)

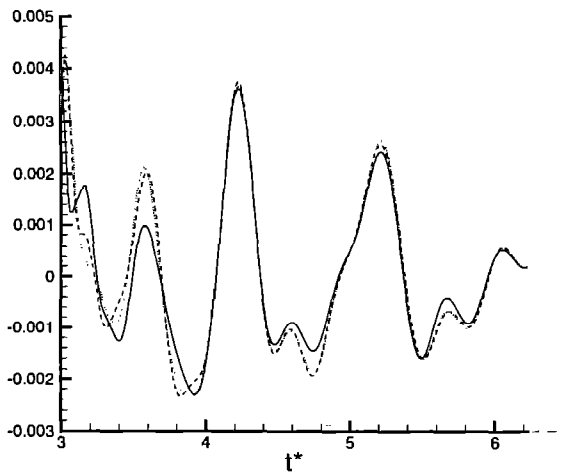

(a)

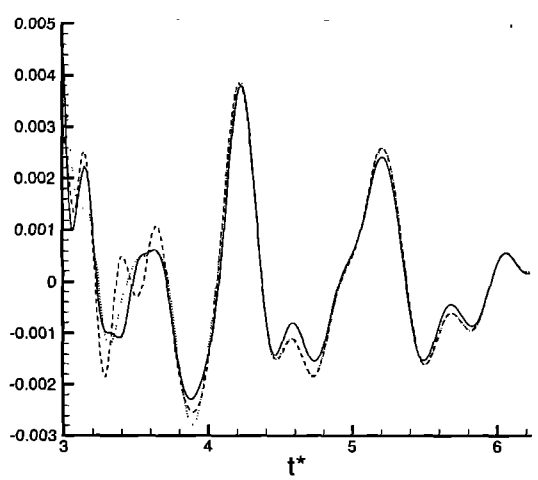

(b)

Fig. 13 Comparison between the fluctuating acoustic pressures — $\widetilde{p'}$, - - p'_{LES} and $\cdots$ $p'_{LES} + \mathcal{P}'_{SGS}$, where p'_{SGS} has been computed from Bardina's model for the Gaussian filter. (a) - $kc = 10$, (b) - $kc = 12$.

The evolution of the intensity ratio $(I_{SGS} - \mathcal{I}_{SGS})/\widetilde{I}$ as a function of k_c is reported on Fig. 14.

The correction on the acoustic intensity ratio obtained using Bardina's model is also relevant, the error

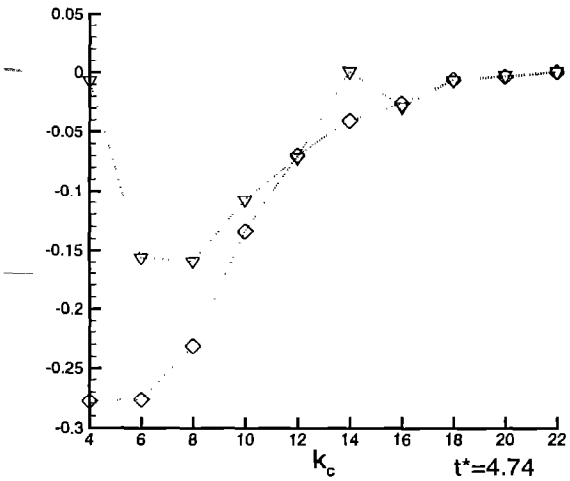

(a)

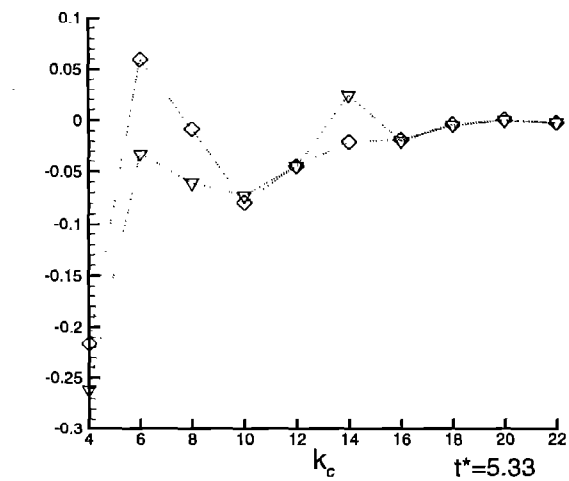

(b)

Fig. 14 Comparison between the subgrid scale intensity $I_{SGS}/\widetilde{I}$, $\diamond$, and the $(I_{SGS} - \mathcal{I}_{SGS})/\widetilde{I}$, ∇ where $\mathcal{I}_{SGS}$ has been computed from Bardina's model with a Gaussian filter as a function of cut-off wave number k_c.

being reduced to [0% - 10%] for all the considered values of the cut-off wave number k_c. The introduction of Bardina's model to estimate the Lighthill's subgrid-scale tensor leads then to more reliable results than with a eddy-viscosity model type. This can be explained by the fact that scale-similarity models are designed to represent the SGS tensor itself (and not a kinetic energy transfer like the eddy-viscosity models), and are known to predict in a very realistic way the eigenvalues and the eigenvectors of the subgrid-scale tensor, as demonstrated by *a priori* tests.[27]

Conclusions

In order to bring out the successive step to obtain subgrid acoustic term for hybrid LES calculation, a

DNS of decaying isotropic turbulence has been carried out. A new Lighthill's equation has been derived from filtered Navier-Stokes equations. The acoustic source term $\frac{\partial^2}{\partial t^2}T_{ij}$ used for DNS computation has been splitted into three parts according to equation (22) : a term $\frac{\partial^2}{\partial t^2}T''_{ij}$ associated to the high frequency part of the acoustic source that is not resolved in LES calculations, the expected source term for LES based on the filtered basic variables $\frac{\partial^2}{\partial t^2}T^{LES}_{ij}$ and a subgrid-scale source term $\frac{\partial^2}{\partial t^2}T^{SGS}_{ij}$.

In order to justify that LES calculations can be used to evaluate acoustic sources, the noise generated by the high frequency part of the source has been estimated and compared to the full noise. Acoustic intensity of the unresolved noise has been computed as a function of the cut-off wavenumber k_c. For usual cut-off wavenumber used in large-eddy simulation, the noise generated by the unresolved acoustic source has been found to be negligeable.
It has been shown that subgrid scale intensity and the subgrid fluctuating acoustic pressure can not be neglected for cut-off wave number used in LES in the present configuration.

As the subgrid scale tensor in Lighthill's equation has the same expression than the subgrid-scale tensor used for fluid computation τ_{ij}, two existing models have been tested. These models are the Smagorinsky model and the Bardina model. Only the Bardina model leads to reliable results.

References

[1]C. K. W. Tam, Computational aeroacoustics : Issues and Methods, *AIAA Journal*, Vol. 33, No 10., 1995

[2]H. S. Ribner, Quadrupole correlations governing the pattern of jet noise, *J. Fluid Mech.*, Vol. 38, pp 1-24, 1969

[3]M. E. Goldstein, B. Rosenbaum, Effects of anisotropic turbulence on aerodynamic noise,*J. Acoust. Soc. Am.*, Vol. 54, pp 630-645, 1973

[4]W. Béchara, P. Lafon, C. Bailly, S. Candel, Application of a $k-\epsilon$ model to the prediction of noise for simple and coaxial free jets. *J. Acoust. Soc. Am.*, Vol. 97, pp 3518-3531, 1995

[5]B. E. Mitchell, S. K. Lele, P. Moin, Direct Computation of Mach Wave Radiation in an Axisymetric Supersonic Jet, *AIAA Journal*, Vol. 35, No 10, 1997

[6]F. Bastin, P. Lafon, S. Candel, Computation of jet mixing noise due to coherent structures : the plane jet case, *J. Fluid Mech.*, Vol. 335, pp 261-304, 1997

[7]C. Bailly, S. Candel, P. Lafon, Prediction of supersonic jet noise from a statistical acoustic model and a compressible turbulence closure, J. of Sound and Vibration **194**(2), pp 219-242, 1996

[8]C. Bailly, P. Lafon, S. Candel, Subsonic and Supersonic Jet Noise Prediction from Statistical Source Models *AIAA Journal*, Vol. 35, No 11, pp 1688-1696, 1997

[9]A.Witkowska, D. Juvé, J.G. Brasseur, Numerical Study of Noise from Isotropic Turbulence, *J. Comp. Acoustics*, Vol. 5, No 3, pp 317-336. (1997)

[10]E. Manoha, B. Troff, P. Sagaut, Trailing Edge Noise Prediction using Large-Eddy Simulation and Acoustic Analogy, *AIAA Paper 98-1066*, Reno, USA, 1998

[11]M. J. Lighthill, On sound generated aerodynamically. Part I : General theory, *Proc. of the Royal Society of London*, Vol. A**211**,pp 564-587 , 1952

[12]M. J. Lighthill, On sound generated aerodynamically. Part II: Turbulence as a source of sound, *Proc. of the Royal Society of London*, Vol. A**222**, pp 1-32, 1954

[13]G. M. Lilley, The generation and radiation of supersonic jet noise. Vol IV - Theory of turbulence generated jet noise, noise radiation from upstream sources and combustion noise. Part II : Generation of sound in a mixing region, *Air Force Aero Propulsion Laboratory* AFAPL-TR-72-53, 1972

[14]A. Favre, Equations statistiques aux fluctuations turbulentes dans les écoulements compressibles : cas des vitesses et des températures, *C. R. Acad. Sciences de Paris* 273, 1971

[15]A. W. Vreman, B. J. Geurts, J. G. Kuerten, P. J. Zandbergen, A finite volume approach to large eddy simulation of compressible, homogeneous, isotropic, decaying turbulence, *Int. J. Numer. Methods Fluids*, Vol 15, pp 799-816, 1992

[16]F. J. Brandsma, Mathematical and physics aspects of simulation based on Navier-Stokes equations, *ISNaS 88.08.024/NL-RTP 89969 L*, 1989

[17]S. Sarkar, G. Erlebacher, M. Y. Hussaini, H. O. Kreiss, The analysis and modelling of dilatation terms in compressible turbulence *J. Fluid Mech.*, Vol. 227, pp 473-493, 1991

[18]M. Lesieur, Turbulence in Fluids, *2nd edn., Kluwer Academic*, 1990

[19]S. Sarkar, M. Y. Hussaini, Computation of the sound generated by isotropic turbulence, *ICASE, Report No 93-74*, 1993

[20]P. Moin, K. Mahesh, Direct Numerical Simulation : A Tool in Turbulence Research, *Ann. Rev. Fluid Mech.* **30**, pp 539-578, 1998

[21]M. Lesieur, O. Métais , New trends in large-eddy simulations of turbulence *Ann. Rev. Fluid Mech.* **28**, pp 45-82, 1996

[22]R.S. Rogallo,P. Moin, Numerical simulation of turbulent flows. *Ann. Rev. Fluid Mech.* **16**, pp 99-137, 1984

[23]J. Smagorinsky, General circulation experiments with primitive equations. I: The basic experiment, *Month. Weath. Rev.* Vol. 91, No 3, pp 99-165, 1963

[24]G. Erlebacher, M. Y. Hussaini, C. G. Speziale, T.A. Zang, Toward the large-eddy simulation of compressible turbulence, *J. Fluid Mech.*, Vol. 238, pp 155-185, 1992

[25]C. G. Speziale, G. Erlebacher,T.A. Zang, M. Y. Hussaini, The subgrid scale modeling of compressible turbulence, *Phy. Fluids* Vol. 31 No 4, pp 940-942, 1988

[26]J. Bardina, J.H. Ferziger, W.C. Reynolds, Improved subgrid scale models for large eddy simulation. *AIAA Paper* 80-1357, 1980

[27]J. Bardina, J.H. Ferziger, W.C. Reynolds, Improved turbulence models based on large eddy simulation of homogeneous, incompressible, turbulent flows, *Report TF-19, Thermosciences Division, Dept. Mechanical Engineering, Stanford University*, 1983